Proton and sodium MRI assessment of emerging tumor chemotherapeutic resistance

Victor D. Schepkin[1,2,*], **Kuei C. Lee**[2], **Kyle Kuszpit**[2], **Mukilan Muthuswami**[2], **Timothy D. Johnson**[3], **Thomas L. Chenevert**[2], **Alnawaz Rehemtulla**[2], and **Brian D. Ross**[2]

[1]National High Magnetic Field Laboratory, Florida State University, Tallahassee, FL 32310, USA

[2]Department of Radiology, Center for Molecular Imaging, University of Michigan Medical School, Ann Arbor, MI 48109-0503, USA

[3]Department of Biostatistics, Center for Molecular Imaging, University of Michigan Medical School, Ann Arbor, MI 48109-0503, USA

Abstract

The ultimate goal of any cancer therapy is to target the elimination of neoplastic cells. Although newer therapeutic strategies are in constant development, therapeutic assessment has been hampered by the inability to assess, rapidly and quantitatively, efficacy *in vivo*. Diffusion imaging and, more recently, sodium MRI have demonstrated their distinct abilities to detect therapy-induced alterations in tumor cellularity, which has been demonstrated to be indicative of therapeutic efficacy. More importantly, both imaging modalities detect tumor response much earlier than traditional methodologies that rely on macroscopic volumetric changes. In this study, the correlation between tumor sodium and diffusion was further tested to demonstrate the sensitivity of sodium imaging to gauge tumor response to therapy by using a 9L rat gliosarcoma treated with varying doses of BCNU [1,3-bis(2-chloroethyl)-1-nitrosourea]. This orthotopic model has been demonstrated to display variability in response to BCNU therapy where initial insult has been shown to lead to drug-resistance. In brief, a single 26.6 mg/kg BCNU dose yielded dramatic responses in both diffusion and sodium MRI. However, a second equivalent BCNU dose yielded a much smaller change in diffusion and sodium, suggesting a drop in tumor sensitivity to BCNU. The MRI responses of animals treated with 13.3 mg/kg BCNU were much lower and similar responses were observed after the initial and secondary applications of BCNU. Furthermore, these results were further validated using volumetric measurements of the tumor and also *ex vivo* determination of tumor sensitivity to BCNU. Overall, these experiments demonstrate the sensitivity and applicability of sodium and diffusion MRI as tools for dynamic assessment of tumor response to therapy.

Keywords

tumor; diffusion; sodium; magnetic resonance imaging; 1,3-bis(2-chloroethyl)-1-nitrosourea; BCNU; chemotherapy resistance

Correspondence to: V. D. Schepkin, National High Magnetic Field Laboratory, 1800 East Paul Dirac Dr., Tallahassee, FL 32310, USA. schepkin@magnet.fsu.edu.

INTRODUCTION

Within solid tumors lies a heterogeneous mass of cells that may exhibit variable growth rates and, more importantly, drug sensitivities that may play a role in the unpredictability of tumor response to therapy. Since tumors are heterogeneous by nature, a tremendous need exists for a standardized approach to benchmark tumor response efficiently and rapidly. To achieve such a feat would provide tremendous gains for preclinical development of experimental therapeutics where novel strategies could be dynamically evaluated throughout treatment. More importantly, there are clear clinical implications where rapid assessment of therapeutic efficacy could lead to opportunities to optimize therapeutic protocols in reaction to changes in tumor response to therapy. In response to this need, diffusion MRI has been demonstrated as a powerful tool for quantitative assessment of tumor response to therapeutic insult by observing the microscopic changes in water diffusion that occur as a result of cellular destruction (1).

A multitude of studies have validated the applicability of diffusion MRI, in both preclinical and clinical models, for providing early assessment of therapeutic efficacy as well as a predictor of therapeutic outcome (2–10). The benefit of diffusion MRI arises from the exploitation of the biophysical property of water diffusion, which is highly sensitive to microscopic changes in cellular structure. Moreover, these microscopic changes precede eventual macroscopic changes in tumor volume, which occur at much later stages after therapeutic insult. Similarly, other biomarkers could potentially be utilized to provide an indication of cellularity such as tissue sodium concentration (TNa). Intracellular and extracellular sodium concentrations are highly regulated during normal physiology; therefore, any disruption in cellular integrity can lead to abnormal imbalances that are detectable using sodium MRI. Since both diffusion and sodium MRI rely on biophysical properties driven by changes in cellular structure, sodium MRI should provide similar reliability and efficiency for assessing tumor response to therapy. Recently, sodium MRI has garnered attention where studies have provided a glimpse into the utility of this approach to observe tumor response to chemotherapy in a variety of model systems (11–13). However, sodium imaging, both technically and its translational application in oncology, has yet to be fully realized and is currently under investigation (14–26).

In this study, sodium and diffusion MRI, applied concurrently, were further explored as tools for providing a quantitative readout of tumor response to therapy. The well-characterized 9L gliosarcoma tumor model has been historically demonstrated to exhibit the emergence of drug resistance in response to initial BCNU [1,3-bis(2-chloroethyl)-1-nitrosourea] therapy (27–31). Using this model system, this study was aimed at ascertaining the correlation between sodium and diffusion imaging and their sensitivity to measure quantitatively tumor responses, which can thereby serve as a sensitive biomarker of therapy-induced cellular changes. By concurrently employing diffusion MRI, the results demonstrated that sodium MRI indeed provided early indication of changes in TNa that paralleled changes in ADC. Moreover, by employing two dosing regimens with groups receiving either two doses of 13.3 mg/kg or 26.6 mg/kg BCNU, both imaging methods were further demonstrated to be highly sensitive in discerning differences in tumor response between both treatment groups, which was later verified by observable differences in tumor volume. In addition, sodium and diffusion imaging detected an apparent shift in BCNU sensitivity due to the emergence of drug resistance, which was confirmed with *ex vivo* BCNU sensitivity assays of tumor samples demonstrating a measurable shift in drug sensitivity. In conclusion, these findings taken together further validate the utility of sodium and diffusion MRI as a quantitative and rapid approach for dynamic assessment of tumor response.

METHODS

Cell culture

Rat 9L gliosarcoma cells (passage 12) from the Brain Tumor Research Center at the University of California at San Francisco were maintained and grown as monolayer cultures in Dulbecco's modified Eagle's medium (DMEM) supplemented with 10% (v/v) heat-inactivated fetal bovine serum, 100 IU/mL penicillin and 100 µg/mL streptomycin at 37°C in a normally humidified atmosphere containing a 95:5 (v/v) air–CO_2 mixture. Prior to implantation, cells were grown to 90% confluence in a 175-cm^2 flask, harvested using a 0.25% trypsin–0.1% EDTA solution and counted using a Coulter cell counter. Cells were pelleted and re-suspended in serum-free DMEM at a concentration of 1×10^5 cells per 10 µL and kept on ice until use. Cell culture reagents were obtained from Invitrogen Life Technologies (Carlsbad, CA, USA).

Tumor implantation

Male Fisher 344 rats ($n = 15$) weighing ~75 g (Harlan, Indianapolis, IN, USA) were anesthetized by intraperitoneal (IP) injection using an 87:13 (v/v) ketamine–xylazine mixture. Under aseptic conditions, 9L cells, prepared as described previously, were injected subcutaneously into the right flank. A total volume of 50 µL was injected, containing approximately 5×10^5 9L cells.

Chemotherapy

Approximately 13 days after tumor implantation, 15 tumor-bearing rats were divided into three parts: five for the control group and two groups of five each for treatment with two different BCNU doses. The average tumor size at the time of treatment (13 days after tumor implantation) in all groups was 380 ± 130 µL. The treated groups received BCNU therapy. A standard 100-mg BCNU preparation (Bristol-Meyers, Princeton, NJ, USA) was dissolved in ethanol and further diluted with 100% saline as recommended by the manufacturer. The freshly prepared BCNU solution was immediately used for single-dose IP injections of 13.3 mg/kg ($1\times$) and 26.6 mg/kg ($2\times$) for the first and second treated animal groups, respectively. In the same fashion, the same doses of BCNU were given again when both tumor ADC and sodium reached pretreatment values. The second BCNU administration was performed in 14 and 21 days after the first intervention for the $1\times$ and $2\times$ groups, respectively. All animal experiments were conducted according to the protocols approved by the University of Michigan Committee on Use and Care of Animals.

Magnetic resonance imaging

Sodium and proton MRI were performed concurrently every 2–3 days on all animals until closure of the experiment when tumors reached an excessive volume. Proton and sodium MR scans were performed using a 9.4-T MR scanner (120-mm clear horizontal bore) (Varian, Palo Alto, CA, USA) and a double-tuned volume RF coil with an internal diameter of 34 mm and length of 65 mm (Doty Scientific, Columbia, SC, USA). Animal body temperature was maintained during MRI scans by using a temperature-controlled circulating water heating pad. Anesthesia was maintained at a 1.25% (v/v) isoflurane–air mixture throughout image acquisitions.

Sodium MRI

The tumor region of the rat was placed at the center of the RF coil. The axial length of the RF coil homogeneous region (deviation $< \pm 5\%$) was approximately 20 mm, which was sufficient to encompass the spatial extent of the tumors and allow quantitative tumor sodium imaging. Because sodium has short T_2 relaxation time components, a 3D back-projection

pulse sequence was used (32). In the original spin-echo 3D back-projection pulse sequence (Varian), two hard pulses provided an echo time of 1000 µs. The other parameters included readout gradient 1.3 G/cm, field of view (FOV) $64 \times 64 \times 64$ mm, 64 complex points in the readout direction using 32×32 projections, repetition time $TR = 0.1$ s and scan time approximately 28 min. The duration of the 90° pulse was 50 µs. In these experiments, the sodium T_1 relaxation time in normal rat muscle was 37 ± 1 ms at 9.4 T, thus yielding an almost unsaturated Na^+ signal during 3D imaging. Reconstructions were performed using the Varian Back-Projection software and Matlab (v. 7.0.1). Data were zero-filled to 256 points prior to Fourier transformation. The final axial output sodium images were made by summing eight adjacent slices together to achieve a comparable slice to slice separation with diffusion proton images.

Proton MRI

The protocol for proton multi-slice diffusion MRI utilized the following parameters: FOV = 40×40 mm, acquisition matrix 128×128, 15 slices, slice thickness = 1.5 mm, slice gap = 0.5 mm, $TR = 3$ s and echo time (TE) = 40 ms. The diffusion spin-echo pulse sequence employed isotropic diffusion weighting by orthogonalization of x-, y- and z-gradient waveforms (33). Specifically, the imaging plus diffusion gradient waveforms were designed to equalize diagonal elements and zero-out off-diagonal elements of the b-matrix. In addition, this sequence included first-order flow compensation and a 32-point navigator echo for motion correction prior to image reconstruction. Diffusion weighted images (DWI) at two-b-factor settings were acquired for calculation of ADC maps: 'high-b' ($b = 1082$ s/ mm^2) and 'low-b' ($b = 117$ s/mm^2). The total diffusion scan time was 18 min. Proton images and ADC maps were reconstructed in Matlab and the tumor volume and average ADC values were determined over a 3D volume of interest (VOI) for each temporal measurement.

Quantification and analysis

Three-dimensional sodium images were co-registered to the target proton multi-slice ADC map image set. Use of a double-tuned coil minimized the demands for the co-registration procedure. This process placed all images on to a common geometric frame, allowing the tumor VOI definition to be performed on available higher quality images. Tumor sodium concentration was determined as an average for all voxels over the 3D tumor volume determined by ADC image at each time point.

For quantification of sodium measurements, sodium MR signals were acquired using adjusted 90° pulses and compared with three references samples consisting of saline solutions with 38, 77 and 154 mM NaCl. The size of these reference samples (diameter × length = 30×65 mm) was chosen to fill the working space of the RF coil. The differences in RF coil loading between animals and between reference samples were determined from duration of the RF pulse required to achieve a sodium 90° flip angle for each animal. The found pulse durations were used during Na signal quantification to correct the difference in coil sensitivity at the different coil loads. Sodium concentrations were presented as mM per volume of tissue detected by MRI.

Each animal had sodium MRI and ADC map measurements performed in axial planes throughout the tumor. Reproducibility of the imaging experimental conditions was assessed by stability of Na^+ signal intensity and ADC measurements in the contra-lateral flank regions. Results of all ADC and sodium concentration measurements are presented as average ± SEM. Tumor volumes were normalized to 1 at the time of treatment.

Ex vivo BCNU sensitivity assay

Tumors were excised from the animals at the end of MRI experiments. Three or more animals were used for the *ex vivo* assay in each group. In the group treated with a 1× dose of BCNU, tumor cells were extracted at day 14 after initiation of therapy. In the group treated with a 2× dose of BCNU, tumor cells were extracted at day 21. Cells from untreated control tumors were taken from animals ~21 days after tumor implantation. *In vitro* resistance tests were performed using the sulforhodamine assay (34). All cell lines were analyzed at the same time to minimize possible errors. Cells were seeded at a density of 4000 cells/well in 96-well plates. After 24 h, the cells were treated with seven dilutions of BCNU ranging from 0.0 to 200 µM. Cells were allowed to grow until the untreated cells reached confluence and then were fixed and stained with sulforhodamine B (SRB). A microtiter colorimetric analysis system (FluorStar, BMG Lab Technologies, Germany) was used to measure the absorbance at 490 nm, which corresponded to the amount of viable cells. Each cell line (control, 1× and 2× BCNU) was assessed four times and yielded the mean ± SEM. The final cell count data for different BCNU concentrations were fitted by exponential decay functions to determine the inhibition parameters IC_{50}.

RESULTS

Sodium and diffusion imaging

Representative images are shown in Fig. 1, demonstrating the effect of BCNU therapy on a 9L subcutaneous tumor as visualized by both sodium and diffusion MR maps over time. As shown in Fig. 1(A), the untreated tumor has lower ADC values than normal muscle and the tumor can be seen as a low-intensity mass on the diffusion image. In contrast, the corresponding sodium image of the untreated tumor displays a distinguishably higher TNa versus normal muscle tissue. However, at day 8 after BCNU treatment, large increases in both ADC and TNa [Fig. 1(B) and (E), respectively] were observed. In addition, tumor response as detected by both sodium and diffusion MRI was very inhomogeneous, which was especially apparent during tumor repopulation [Fig. 1(C) and (F)]. Therefore, in order to monitor therapeutic efficacy throughout the time course, only the average values of TNa and ADC throughout the tumor were used.

Tumor diffusion

The dynamic changes in tumor ADC as detected by diffusion MRI during the treatment course of a 9L rat subcutaneous tumor using two different doses of BCNU were quantified and are presented in Fig. 2. ADC values in untreated control tumors remained relatively constant [$(1.04 \pm 0.02) \times 10^{-3}$ mm^2/s] throughout the experiment. However, a modest increase of tumor ADC up to $(1.34 \pm 0.02) \times 10^{-3}$ mm^2/s was detected 6 days after treatment with 1× dose of BCNU [Fig. 2(A)]. The estimated rate of ADC increase during 3 days after the initial 1× dose of BCNU was $(0.06 \pm 0.02) \times 10^{-3}$ mm^2/s/day. A second equivalent dose of BCNU was administered on day 14 and yielded another ADC maximum of $(1.31 \pm 0.06) \times 10^{-3}$ mm^2/s at approximately 5 days after the second intervention with a corresponding initial rate of ADC increase at the level of $(0.08 \pm 0.02) \times 10^{-3}$ mm^2/s/day [Fig. 2(A)]. Neither the maximum change nor the rate of change between the two interventions were statistically different ($p > 0.05$).

Using the 2× BCNU dose, a dramatically different response was observed [Fig. 2(B)]. The first administration of BCNU produced a very intense increase in tumor ADC from the non-treated value of $(1.04 \pm 0.02) \times 10^{-3}$ mm^2/s up to a maximum of $(1.87 \pm 0.06) \times 10^{-3}$ mm^2/s at day 9 post-treatment. Moreover, a higher average rate of increase in ADC, compared with the 1× dose BCNU treatment, was found: $(0.12 \pm 0.025) \times 10^{-3}$ mm^2/s/day. Upon reaching the initial ADC value and at the onset of tumor re-growth on day 21, a second

equivalent dose of BCNU (2×) was administered. A considerably reduced rate of tumor ADC increase of $(0.05 \pm 0.01) \times 10^{-3}$ mm^2/s/day) was observed compared with the rate detected subsequent to the initial dose of BCNU and only a fraction of the previous ADC maximum of $(1.20 \pm 0.03) \times 10^{-3}$ mm^2/s was achieved. These data reveal a significant change in both the rate of change and maximum diffusion change between the two doses indicating that a reduced sensitivity to BCNU (i.e. gain of resistance) had occurred following the initial treatment dose. The second maximum ADC in this case was detected ~5 days after the treatment. For comparison, the mean ADC values in contra-lateral normal flank tissue, which were measured at the same time as the tumor values, remained at the level of $(1.27 \pm 0.02) \times 10^{-3}$ mm^2/s for both doses of BCNU therapy.

Tumor sodium

The time courses of TNa as detected by sodium MRI throughout therapy with either 1× or 2× doses of BCNU are shown in Fig. 3. The initial level of sodium in untreated tumors was found to be 43.0 ± 0.6 mM. For comparison, the Na$^+$ concentration in contra-lateral normal flank tissue was 21.1 ± 0.9 mM.

When a 1× dose of BCNU was given, TNa within the tumor increased at an initial rate of 4.1 ± 0.5 mM/day and reached a maximum of 63.2 ± 4 mM on day 5 post-treatment [Fig. 3(A)]. Following a second 1× dose of BCNU, a similar pattern of TNa change was observed, mimicking the rate of change (4.30 ± 1 mM/day) and maximum increase (60.0 ± 4 mM) that was observed from the initial administration of BCNU. More importantly, changes in TNa over time due to the therapeutic insult were highly correlative with changes in ADC within the same time frame.

Using a 2× dose of BCNU, a similar pattern of TNa change [Fig. 3(B)] over time was observed as detected earlier for ADC [Fig. 2(B)]. The first BCNU injection produced a dramatic increase in TNa with an initial rate of 9.8 ± 1.3 mM/day and a maximum of TNa (104 ± 14 mM) was reached at day 8. The average tumor sodium content returned to the pretreatment level in ~21 days, which is comparable to the time course detected by diffusion MRI. The second 2× dose of BCNU treatment yielded a greatly diminished response, as evidenced by a greatly depressed increase in TNa [Fig. 2(B)]. The maximum tumor TNa was not clearly distinguishable as a slow tumor TNa increase usually observed in untreated tumors at the late stages of tumor growth.

Tumor volume

In order to validate our diffusion and sodium MRI findings and to ascertain the utility of each approach for assessing therapeutic efficacy, volumetric measurements over the course of therapy were obtained to observe discernible changes in tumor growth kinetics. A comparison of the changes in tumor volumes in the control group versus changes in tumor volumes in the treated groups is shown in Fig. 4. Tumor volume in the untreated group increased quickly by 8-fold in ~9 days with a volumetric doubling time of 3.1 ± 0.5 days. Treatment of tumors with the first 1× dose of BCNU resulted in an 8-day tumor growth delay. Following the second 1× dose of BCNU, a more pronounced decrease in tumor doubling time (9.3 ± 0.8 days) was found versus control tumors as determined by fitting of the volumetric data to an exponential function.

In the group that received a 2× dose of BCNU, significant growth inhibition was detectable as the tumor increased less than 2-fold at 10 days post-onset of therapy [Fig. 4(B)] which was followed by a decrease in volume until day 19, at which time tumor re-growth began. At this time, a second equivalent dose of BCNU was administered that further delayed tumor growth until day 30. Interestingly, as is apparent in Fig. 4(B), the second dose of 2×

BCNU produced a diminished growth delay compared with the initial dose of BCNU, suggesting that perhaps the tumor was less sensitive to the second dose.

Ex vivo assessment of tumor BCNU resistance

To provide insight into tumor responsiveness after BCNU therapy, tumors from each group were excised and tested for alteration in BCNU sensitivity. For untreated control tumors, the IC_{50} was found to be 42 ± 5 µM (Table 1). When tumors were treated with a $1\times$ dose of BCNU, increased resistance to BCNU was revealed ($IC_{50} = 54 \pm 4$ µM, Table 1), which was not statistically different from the control ($p > 0.05$). In the case of animals receiving a $2\times$ dose of BCNU (Table 1), a significant resistance to BCNU was detected as shown by a nearly 50% increase in IC_{50} ($IC_{50} = 62 \pm 1$ µM, $p < 0.01$) compared with untreated controls.

DISCUSSION

Current methods for assessing tumor response to therapy rely mainly on macroscopic changes in volume or alterations in survival as markers of efficacy, which require a significant time for these outcomes to be achieved. A tremendous need exists for rapid and noninvasive quantitative imaging of therapeutic response; such methods could both play a key role in preclinical studies and provide huge advantages in the clinical setting. Furthermore, imaging approaches offer great potential for individualizing treatment response monitoring, thus transitioning towards the tailoring of patient treatments. In response to this goal, diffusion MRI has been proven to be a useful and sensitive tool for assessment of tumor response to therapy in preclinical models (2,8–10,35). More importantly, diffusion MRI has already taken the leap into clinical applications and has shown great promise for predicting therapeutic outcome well in advance of current methods (6,7). More recently, sodium MRI has also been demonstrated to provide early detection of response to therapy in various animal models by detecting changes in TNa during cell death and it has been shown to be highly correlative with diffusion MRI (12,13).

In this study, we aimed to expand further our investigation of diffusion and sodium imaging as viable biomarkers of cancer therapy. The marginal difference between tumor sensitivity and systemic toxicity continues to pose a dilemma for therapeutic strategies. The problem is exacerbated when alterations within the tumor may occur during fractionated dosage schedules, leading to a decrease in therapeutic effectiveness of the current regimen. Hence it is imperative to be able to monitor rapidly changes in therapeutic efficacy and to detect these changes over time and in individual subjects. To determine whether diffusion and sodium MRI could provide a sensitive readout to detect changes in tumor response to therapy, we employed the 9L gliosarcoma model and various BCNU treatment regimens. Using a BCNU dose of $1\times$, our results demonstrated that sodium MRI was able to detect rapidly tumor response to BCNU therapy [Fig. 3(A)], which correlated highly with concurrent diffusion data [Fig. 2(A)]. When a larger chemotherapeutic dose ($2\times$) was used, a much greater tumor response was detected after the initial administration of the drug and a strong correlation was again shown to exist between sodium and diffusion imaging. These findings were also validated by observing tumor growth kinetics, which confirmed that treatment with a low dose of BCNU did indeed provide improved tumor control and a higher dose of BCNU provided even greater therapeutic benefit. Interestingly, our data suggested that treatment with BCNU led to changes in tumor sensitivity to BCNU, which was especially apparent when a $2\times$ dose of BCNU was given to the animals. In comparison, a low dose of BCNU ($1\times$) produced a similar response, as detected by diffusion and sodium MRI, after both the initial and subsequent dose of BCNU.

Furthermore, representative tumors were excised at the end of MRI experiments from both $1\times$ and $2\times$ treated groups to generate cell lines for testing BCNU sensitivity. As previously

described, the 1× doses of BCNU produced similar responses whether after the initial dose or the second dose (Figs 2 and 3). Using the SRB growth inhibition assay, tumors taken after the second dose were shown to have somewhat increased BCNU resistance, which correlated with similar responsiveness as detected by sodium and diffusion MRI. Interestingly, a 2× dose of BCNU produced a much higher response after the initial dose, but a subsequent equivalent dose produced a greatly diminished response as quantified by sodium and diffusion MRI. Chemo-sensitivity testing revealed that tumors which received two high doses of therapy had a much greater resistance to BCNU, which was suggested earlier by both sodium and diffusion MRI experiments. This observation is consistent with historical findings that treatment of 9L tumors with BCNU does indeed lead to the emergence of drug resistance (28,36). These data taken together, including *ex vivo* BCNU sensitivity assays on excised tumors, validated the hypothesis that shifts in BCNU sensitivity occur during treatment, and that they are detectable using sodium and diffusion MRI.

CONCLUSION

The results of this study demonstrate the coherent ability of diffusion and sodium MRI to reveal the efficacy of tumor therapy in a few days following treatment in a dose-dependent manner. The emerging tumor resistance to BCNU was detected by both imaging modalities and was confirmed by *ex vivo* assay of tumor cells derived from *in vivo* treated tumors. Correlation between diffusion and sodium continues to be present during alterations in tumor sensitivity to treatment. These results support current clinical trials of ADC as an indicator of tumor cellularity during cancer therapy and demonstrate the complementary insights of ^{23}Na MRI for tumor assessments to treatment intervention. Finally, application of sodium MRI may prove invaluable, especially in situations where tissue motion can not be easily minimized.

Acknowledgments

Abbreviations used

1×	dose of BCNU 13.3 mg/kg
2×	dose of BCNU 26.6 mg/kg
ADC	apparent diffusion coefficient
BCNU	1,3-bis(2-chloroethyl)-1-nitrosourea
FOV	field of view
IC$_{50}$	inhibition of cells counted at the 50% level
IP	intraperitoneal
SRB	sulforhodamine B
TNa	tissue sodium concentration

VOI volume of interest

REFERENCES

1. Ross BD, Chenevert TL, Kim B, Ben-Yoseph O. Magnetic resonance imaging and spectroscopy: application to experimental neurooncology. Q. Magn. Reson. Biol. Med. 1994; 1:89–106.

2. Chenevert TL, McKeever PE, Ross BD. Monitoring early response of experimental brain tumors to therapy using diffusion magnetic resonance imaging. Clin. Cancer Res. 1997; 3:1457–1466. [PubMed: 9815831]

3. Chenevert TL, Meyer CR, Moffat BA, Rehemtulla A, Mukherji SK, Gebarski SS, Quint DJ, Robertson PL, Lawrence TS, Junck L, Taylor JM, Johnson TD, Dong Q, Muraszko KM, Brunberg JA, Ross BD. Diffusion MRI: a new strategy for assessment of cancer therapeutic efficacy. Mol. Imaging. 2002; 1:336–343. [PubMed: 12926229]

4. Chenevert TL, Stegman LD, Taylor JM, Robertson PL, Greenberg HS, Rehemtulla A, Ross BD. Diffusion magnetic resonance imaging: an early surrogate marker of therapeutic efficacy in brain tumors. J. Natl. Cancer Inst. 2000; 92:2029–2036. [PubMed: 11121466]

5. Gillies RJ, Raghunand N, Karczmar GS, Bhujwalla ZM. MRI of the tumor microenvironment. J. Magn. Reson. Imaging. 2002; 16:430–450. [PubMed: 12353258]

6. Hamstra DA, Chenevert TL, Moffat BA, Johnson TD, Meyer CR, Mukherji SK, Quint DJ, Gebarski SS, Fan X, Tsien CI, Lawrence TS, Junck L, Rehemtulla A, Ross BD. Evaluation of the functional diffusion map as an early biomarker of time-to-progression and overall survival in high-grade glioma. Proc. Natl. Acad. Sci. USA. 2005; 102:16759–16764. [PubMed: 16267128]

7. Moffat BA, Chenevert TL, Lawrence TS, Meyer CR, Johnson TD, Dong Q, Tsien C, Mukherji S, Quint DJ, Gebarski SS, Robertson PL, Junck LR, Rehemtulla A, Ross BD. Functional diffusion map: a noninvasive MRI biomarker for early stratification of clinical brain tumor response. Proc. Natl. Acad. Sci. USA. 2005; 102:5524–5529. [PubMed: 15805192]

8. Ross BD, Chenevert TL, Rehemtulla A. Magnetic resonance imaging in cancer research. Eur. J. Cancer. 2002; 38:2147–2156. [PubMed: 12387840]

9. Ross BD, Moffat BA, Lawrence TS, Mukherji SK, Gebarski SS, Quint DJ, Johnson TD, Junck L, Robertson PL, Muraszko KM, Dong Q, Meyer CR, Bland PH, McConville P, Geng H, Rehemtulla A, Chenevert TL. Evaluation of cancer therapy using diffusion magnetic resonance imaging. Mol. Cancer Ther. 2003; 2:581–587. [PubMed: 12813138]

10. Zhao M, Pipe JG, Bonnett J, Evelhoch JL. Early detection of treatment response by diffusion-weighted ^{1}H-NMR spectroscopy in a murine tumour *in vivo*. Br. J. Cancer. 1996; 73:61–64. [PubMed: 8554985]

11. Babsky AM, Hekmatyar SK, Zhang H, Solomon JL, Bansal N. Application of 23Na MRI to monitor chemotherapeutic response in RIF-1 tumors. Neoplasia. 2005; 7:658–666. [PubMed: 16026645]

12. Schepkin VD, Chenevert TL, Kuszpit K, Lee KC, Meyer CR, Johnson TD, Rehemtulla A, Ross BD. Sodium and proton diffusion MRI as biomarkers for early therapeutic response in subcutaneous tumors. Magn. Reson. Imaging. in press.

13. Schepkin VD, Ross BD, Chenevert TL, Rehemtulla A, Sharma S, Kumar M, Stojanovska J. Sodium magnetic resonance imaging of chemotherapeutic response in a rat glioma. Magn. Reson. Med. 2005; 53:85–92. [PubMed: 15690506]

14. Ouwerkerk R, Bleich KB, Gillen JS, Pomper MG, Bottomley PA. Tissue sodium concentration in human brain tumors as measured with ^{23}Na MR imaging. Radiology. 2003; 227:529–537. [PubMed: 12663825]

15. Thulborn KR, Davis D, Adams H, Gindin T, Zhou J. Quantitative tissue sodium concentration mapping of the growth of focal cerebral tumors with sodium magnetic resonance imaging. Magn. Reson. Med. 1999; 41:351–359. [PubMed: 10080284]

16. Boada FE, Gillen JS, Shen GX, Chang SY, Thulborn KR. Fast three dimensional sodium imaging. Magn. Reson. Med. 1997; 37:706–715. [PubMed: 9126944]

17. Clayton DB, Lenkinski RE. MR imaging of sodium in the human brain with a fast three-dimensional gradient-recalled-echo sequence at 4 T. Acad. Radiol. 2003; 10:358–365. [PubMed: 12678174]

18. Christensen JD, Barrere BJ, Boada FE, Vevea JM, Thulborn KR. Quantitative tissue sodium concentration mapping of normal rat brain. Magn. Reson. Med. 1996; 36:83–89. [PubMed: 8795025]

19. Kline RP, Wu EX, Petrylak DP, Szabolcs M, Alderson PO, Weisfeldt ML, Cannon P, Katz J. Rapid *in vivo* monitoring of chemotherapeutic response using weighted sodium magnetic resonance imaging. Clin. Cancer Res. 2000; 6:2146–2156. [PubMed: 10873063]

20. Kohler S, Preibisch C, Nittka M, Haase A. Fast three-dimensional sodium imaging of human brain. Magma. 2001; 13:63–69. [PubMed: 11502419]

21. Steidle G, Graf H, Schick F. Sodium 3-D MRI of the human torso using a volume coil. Magn. Reson. Imaging. 2004; 22:171–180. [PubMed: 15010109]

22. Bartha R, Lee TY, Hogan MJ, Hughes S, Barberi E, Rajakumar N, Menon RS. Sodium T_2^*-weighted MR imaging of acute focal cerebral ischemia in rabbits. Magn. Reson. Imaging. 2004; 22:983–991. [PubMed: 15288139]

23. Rooney WD, Springer CS Jr. A comprehensive approach to the analysis and interpretation of the resonances of spins 3/2 from living systems. NMR Biomed. 1991; 4:209–226. [PubMed: 1751345]

24. Foy BD, Burstein D. Characteristics of extracellular sodium relaxation in perfused hearts with pathologic interventions. Magn. Reson. Med. 1992; 27:270–283. [PubMed: 1461113]

25. Jacobs MA, Ouwerkerk R, Wolff AC, Stearns V, Bottomley PA, Barker PB, Argani P, Khouri N, Davidson NE, Bhujwalla ZM, Bluemke DA. Multiparametric and multinuclear magnetic resonance imaging of human breast cancer: current applications. Technol. Cancer Res. Treat. 2004; 3:543–550. [PubMed: 15560711]

26. Glickson JD. Clinical NMR spectroscopy of tumors. Current status and future directions. Invest. Radiol. 1989; 24:1011–1016. [PubMed: 2691439]

27. Black PM. Brain tumor. Part 2. N. Engl. J. Med. 1991; 324:1555–1564. [PubMed: 2027359]

28. Barker M, Hoshino T, Gurcay O, Wilson CB, Nielsen SL, Downie R, Eliason J. Development of an animal brain tumor model and its response to therapy with 1,3-bis(2-chloroethyl)-1-nitrosourea. Cancer Res. 1973; 33:976–986. [PubMed: 4703128]

29. Bredel M, Zentner J. Brain-tumour drug resistance: the bare essentials. Lancet Oncol. 2002; 3:397–406. [PubMed: 12142169]

30. Bredel M, Bredel C, Sikic BI. Genomics-based hypothesis generation: a novel approach to unravelling drug resistance in brain tumours? Lancet Oncol. 2004; 5:89–100. [PubMed: 14761812]

31. Joy A, Panicker S, Shapiro JR. Altered nuclear localization of bax protein in BCNU-resistant glioma cells. J. Neurooncol. 2000; 49:117–129. [PubMed: 11206007]

32. Lauterbur PC. Image formation by induced local interactions: examples employing nuclear magnetic resonance. Nature. 1973; 242:190–191.

33. Moffat BA, Hall DE, Stojanovska J, McConville PJ, Moody JB, Chenevert TL, Rehemtulla A, Ross BD. Diffusion imaging for evaluation of tumor therapies in preclinical animal models. Magma. 2004; 17:249–259. [PubMed: 15580371]

34. Skehan P, Storeng R, Scudiero D, Monks A, McMahon J, Vistica D, Warren JT, Bokesch H, Kenney S, Boyd MR. New colorimetric cytotoxicity assay for anticancer-drug screening. J. Natl. Cancer Inst. 1990; 82:1107–1112. [PubMed: 2359136]

35. Stegman LD, Rehemtulla A, Hamstra DA, Rice DJ, Jonas SJ, Stout KL, Chenevert TL, Ross BD. Diffusion MRI detects early events in the response of a glioma model to the yeast cytosine deaminase gene therapy strategy. Gene Ther. 2000; 7:1005–1010. [PubMed: 10871748]

36. Saito R, Bringas J, Mirek H, Berger MS, Bankiewicz KS. Invasive phenotype observed in 1,3-bis(2-chloroethyl)-1-nitrosourea-resistant sublines of 9L rat glioma cells: a tumor model mimicking a recurrent malignant glioma. J. Neurosurg. 2004; 101:826–831. [PubMed: 15540922]
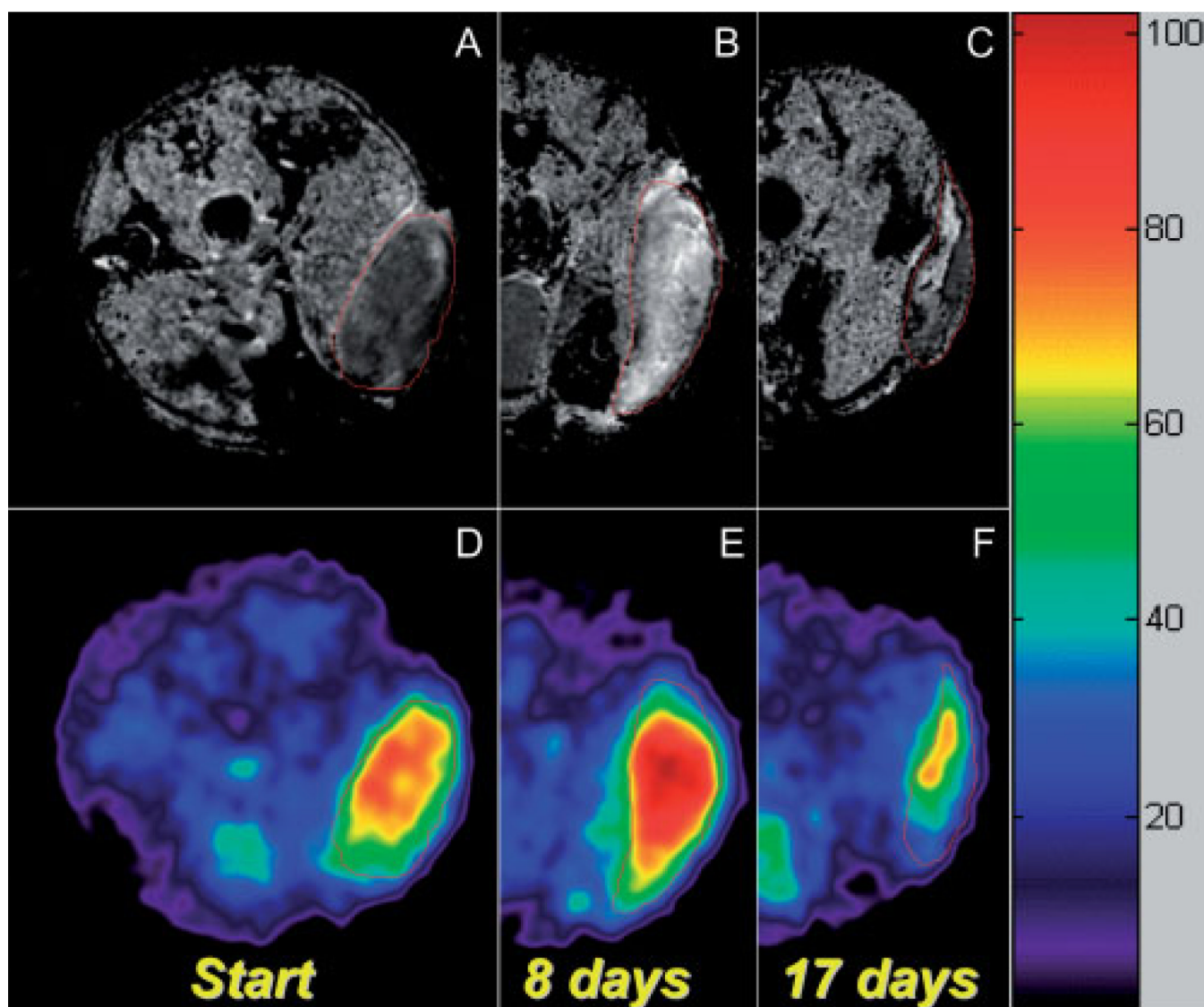
Figure 1.
Proton ADC mapping (A–C) and corresponding co-registered sodium MR images (D–F) of
a 9L rat subcutaneous tumor following BCNU chemotherapy. The images were taken from
the same animal at different time points after a single 2× (26.6 mg/kg) dose of BCNU: the
images of the pretreated tumor are shown at the left (A, D), and are followed by the images
taken at days 8 and 17 after initiation of therapy. Heterogeneous tumor ADC and tumor
sodium can be seen at day 8 post-treatment. At day 17, tumor re-population can be seen as a
reduced (low-diffusion) intensity region within the tumor on the ADC map, which also
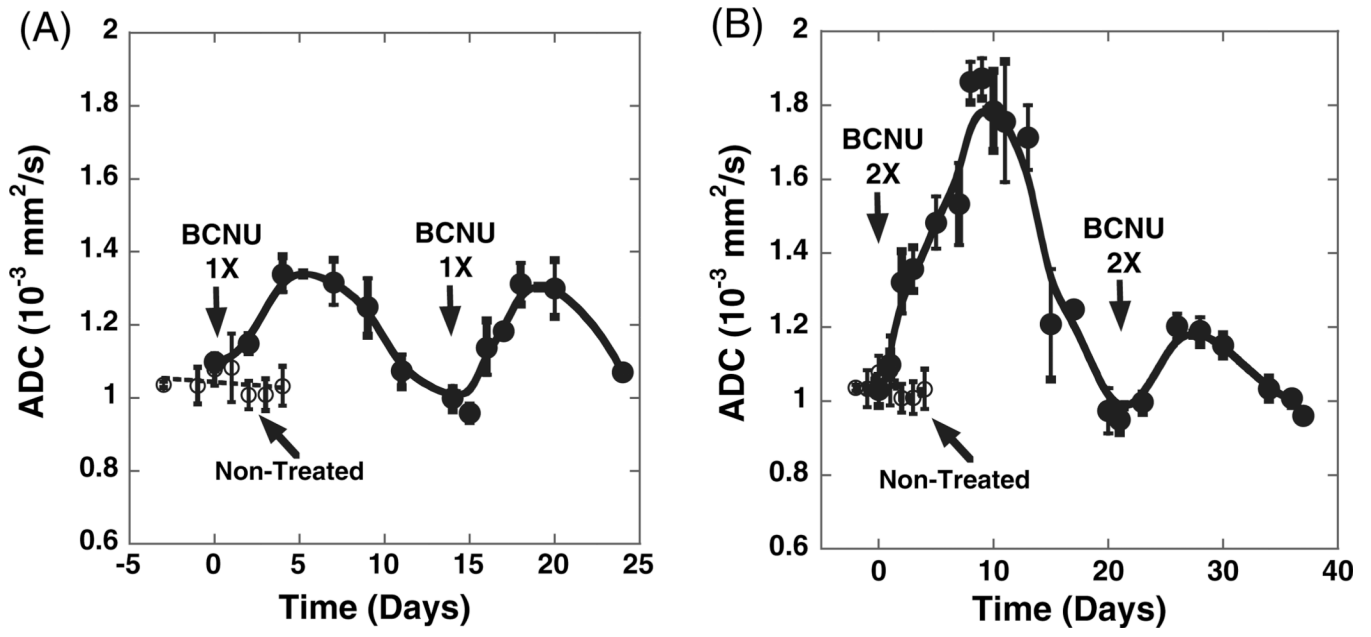corresponds to the low Na^+ concentration on the ^{23}Na MR image.

Figure 2.
Changes in tumor diffusion throughout BCNU therapy. BCNU-treated (●) and untreated controls (○). BCNU doses were (A) 1× = 13.3 mg/kg and (B) 2× = 26.6 mg/kg.
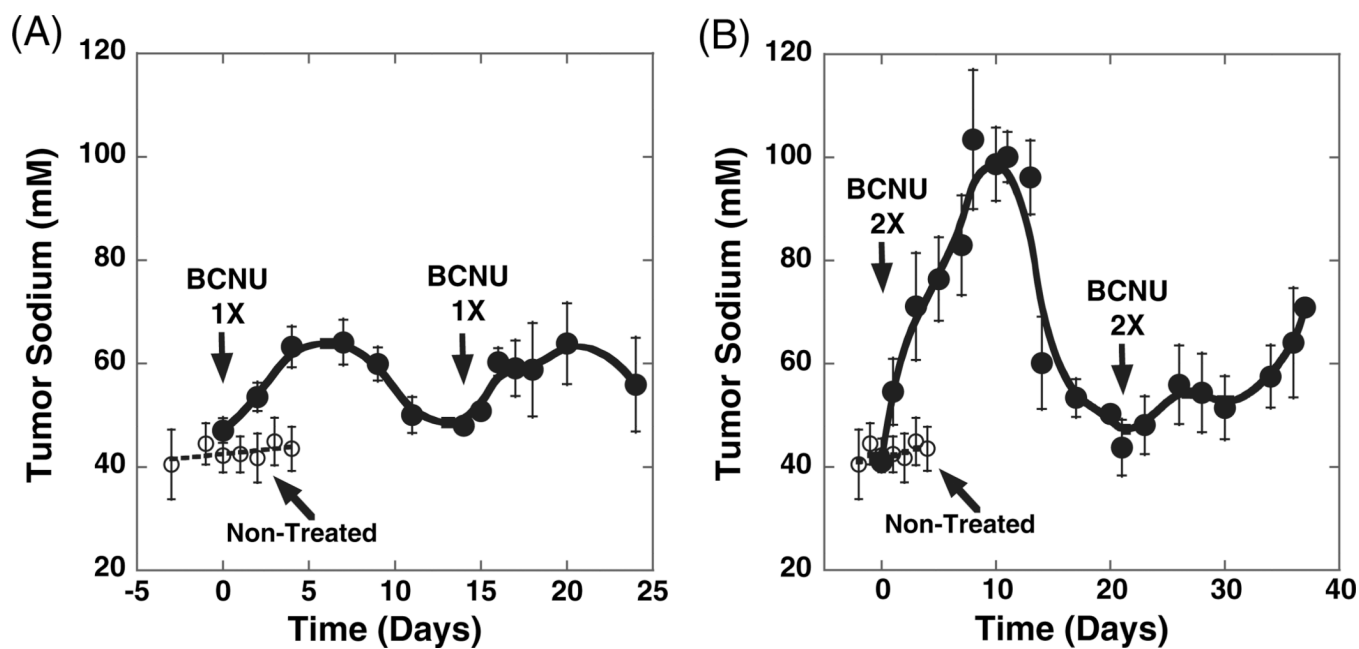
Figure 3.
Changes in tumor sodium throughout BCNU therapy. BCNU-treated (●) and untreated controls (○). BCNU doses were (A) 1×= 13.3 mg/kg and (B) 2× = 26.6 mg/kg.
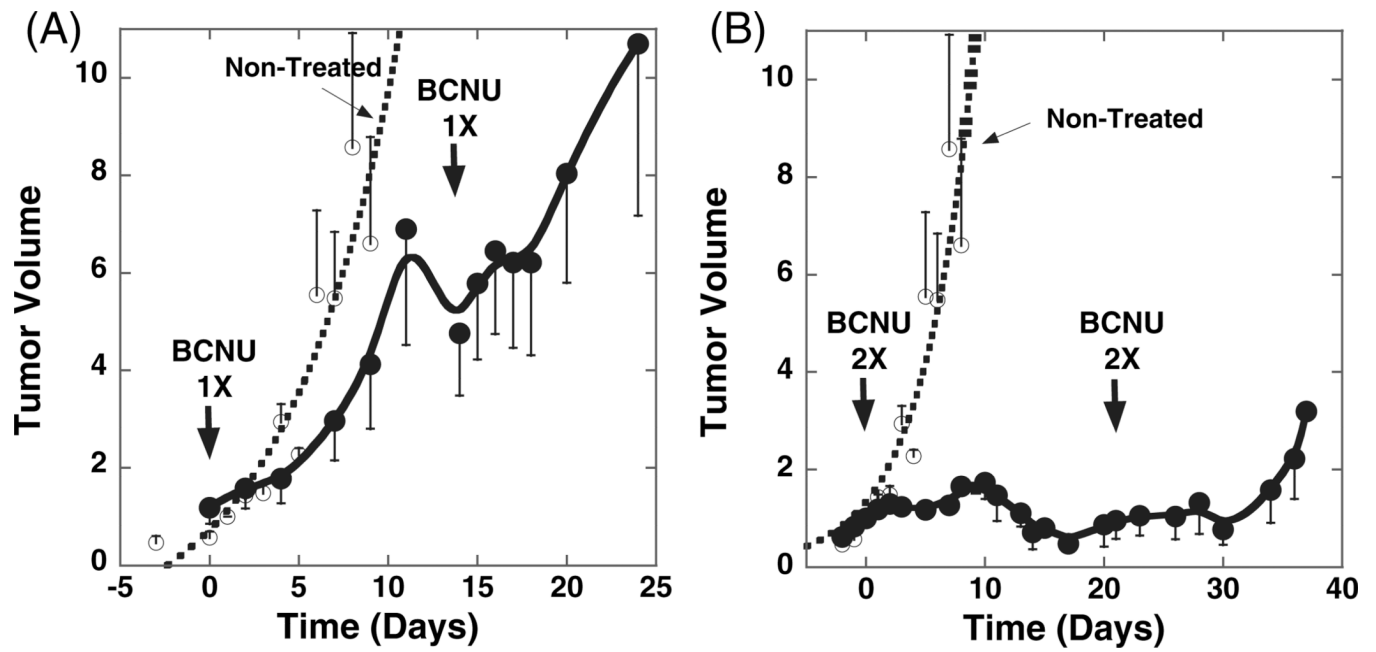
Figure 4.
Volumetric tumor growth measurements over time. BCNU-treated (●) and untreated
controls (○). Tumor volumes were normalized to 1 at the time of treatment. BCNU doses
were (A) 1× = 13.3 mg/kg and (B) 2× = 26.6 mg/kg.

Table 1

Ex vivo determination of BCNU sensitivity[a]

	Control	1× (dose 1)	2× (dose 1)
$IC_{50} \pm SEM$ (µM)	42 ± 5	54 ± 4	62 ± 1
p (versus control)	—	>0.05	<0.01

[a]Cell lines from tumors excised from control, 1× treated and 2× treated animals were assayed using an SRB growth inhibition assay to determine sensitivity to BCNU. The calculated mean $IC_{50} \pm SE$ for control ($n = 6$), 1× ($n = 3$) and 2× ($n = 3$) are shown, and also *p*-values determined using a standard Student's *t*-test.